Measured Magnetic Moments and Shape Coexistence in the Neutron-Deficient Nuclei ^{184,186,188}Pt

A. E. Stuchbery, S. S. Anderssen, A. P. Byrne, P. M. Davidson, G. D. Dracoulis, and G. J. Lane
Department of Nuclear Physics, Research School of Physical Sciences and Engineering, The Australian National University, Canberra, ACT 0200, Australia
(Received 22 December 1995)

A novel implantation-decay technique has been employed to measure the magnetic moments of the 2_1^+ states in the neutron-deficient nuclei ^{184}Pt, ^{186}Pt, and ^{188}Pt. The magnetic moment systematics for the even Pt isotopes now extend from $^{184}_{78}\mathrm{Pt}_{106}$ to $^{198}_{78}\mathrm{Pt}_{120}$, spanning the upper half of the valence neutron shell. Despite the prolate-to-oblate shape transition near $A = 190$, they remain remarkably constant. The $g(2_1^+)$ values for ^{184,186,188}Pt are consistent with shape-coexistence models in which the deformed configuration has a larger effective number of valence protons than the less-deformed configuration.

PACS numbers: 21.10.Ky, 23.20.En, 27.70.+q

Magnetic moments have played an important role in the elucidation of nuclear structure. The magnetic dipole properties of a collective nucleus are sensitive to differences in the behavior of the proton and neutron "fluids," while the electric quadrupole properties depend on their average behavior. As such, magnetic moments provide a perspective on nuclear structure which may complement other measurements and discriminate between different theoretical approaches. The relative difficulty of measuring the magnetic moment, however, often limits experimental studies to favorable cases. In heavy, *unstable* nuclei very few measurements have been made for short-lived excited states (i.e., states with subnanosecond lifetimes). To address this problem we have developed an experimental technique that will enable more comprehensive studies of magnetic moment systematics for low-excitation states in heavy, neutron-deficient nuclei. This Letter reports the first measurements of the 2_1^+ state g factors in the neutron-deficient nuclei ^{184}Pt, ^{186}Pt, and ^{188}Pt. The new data extend the magnetic moment systematics for the even platinum isotopes across the upper half of the valence neutron shell, from ^{184}Pt to ^{198}Pt.

Magnetic moment measurements of short-lived states ($\tau < 1$ ns) in heavy, unstable nuclei present an experimental challenge for several reasons: (i) Because of the short state lifetimes, a measurable precession may be obtained only if the integral perturbed angular correlation and distribution (IPAC/D) technique [1] is employed in conjunction with the intense hyperfine fields $\sim$100 T present at dilute impurities implanted into ferromagnetic hosts. (ii) The heavy-ion beams, required to create the nuclei and implant them during recoil into a ferromagnetic host placed behind a target foil, also interact with the ferromagnetic host, producing background radiation which often obscures the γ-ray decays of interest. (iii) If the reaction leads to the population of many levels in cascade, the observed precessions may reflect the complex feeding paths rather than the precession of an individual level.

Our implantation-decay technique avoids these difficulties. The products of heavy-ion reactions are recoil implanted into iron hosts as usual; however, the implanted nuclei are not those of direct interest, but rather their β-decay parents. After sufficient activity is built up, a multidetector array is used out of beam to measure perturbed γ-γ angular correlations in the daughter nuclei. This method is new in that it combines the conventional "implantation" and "radioactivity" techniques [1] with the sensitivity of a multidetector array.

In the present study, measurements were performed for each of the nuclei ^{184,186,188,190,192}Pt using beams from the ANU 14UD Pelletron accelerator. Experimental details are summarized in Table I. The measurement on the naturally occurring nuclide ^{192}Pt provided both a check of the experimental technique and a calibration of the effective hyperfine magnetic field strength. (The 2_1^+ state g factor and lifetime have been measured previously [2,3].) The ^{190}Pt experiment was discontinued once it was established that a more precise result would be obtained using the transient field technique with a target enriched to 4% in ^{190}Pt [3].

The Fe-backed targets were irradiated at a distance of about 3 m from the γ-ray detector array Caesar [4], configured with seven Compton-suppressed, Ge γ-ray detectors in a (vertical) plane. The seven detectors and their angular placements give 21 two-detector combinations for γ-γ coincidences which may be grouped into six effective detector-detector angles: 14°, 34°, 49°, 63°, 70°, and 83°. After an appropriate irradiation period, the implanted

TABLE I. Experimental particulars.

Nuclide	Reaction	E_{beam} [a] (MeV)	T_{cyc} [a] (h)	T_{run} [a] (d)
^{192}Pt	$^{181}\mathrm{Ta}(^{16}\mathrm{O}, 5n)^{192}\mathrm{Tl}(\beta^+)$	100	2	6
^{190}Pt	$^{170}\mathrm{Er}(^{25}\mathrm{Mg}, 5n)^{190}\mathrm{Hg}(\beta^+)$	128	1	1
^{188}Pt	$^{169}\mathrm{Tm}(^{24}\mathrm{Mg}, 5n)^{188}\mathrm{Tl}(\beta^+)$	128	0.33	6
^{186}Pt	$^{173}\mathrm{Yb}(^{19}\mathrm{F}, 6n)^{186}\mathrm{Au}(\beta^+)$	112	0.33	4
^{184}Pt	$^{165}\mathrm{Ho}(^{24}\mathrm{Mg}, 5n)^{184}\mathrm{Au}(\beta^+)$	128	0.06	7

[a]Beam energy, E_{beam}; cycle time (half irradiation, half counting), T_{cyc}; run duration, T_{run}.

 0031-9007/96/76(13)/2246(4)$10.00

Fe foil was transported to the center of the array using a "rabbit" [5]. The foil was polarized perpendicular to the detection plane using small, permanent, NdFeB magnets and the perturbed γ-γ angular correlations were measured. Irradiation and counting cycles were repeated until sufficient statistical precision was achieved. To reduce possible systematic errors, the direction of the polarizing field was reversed at least once during each experiment.

For each γ-γ cascade we have four independent measures of the perturbed angular correlation $W(\theta, B)$. Two arise from reversing the direction of the magnetic field ($\pm B$) and two from interchanging the γ-ray transitions examined in each detector of the pair ($\pm\theta$):

$$W(\pm\theta, \pm B) = \sum_{k=0,2,4} \frac{b_k \cos[k(\pm\theta \mp \Delta\theta_k)]}{\sqrt{1 + (k\omega\tau)^2}}, \quad (1)$$

where $\omega = -g(\mu_N/\hbar)B$, $\tan(k\Delta\theta_k) = k\omega\tau$, and the coefficients b_k have specified values [1]. The four angular correlations were fitted simultaneously to determine the precession angle $\omega\tau$, an overall normalization parameter, and a factor reflecting the ratio of counting times for "field up" to "field down." For graphical presentation it is convenient to combine the data using the fact that $W(+\theta, +B) = W(-\theta, -B)$ and $W(+\theta, -B) = W(-\theta, +B)$. The two resultant angular correlations may then be referred to as field up and field down, with θ always positive.

Figure 1 shows the data and fits for the $0_2^+ \rightarrow 2_1^+ \rightarrow 0_1^+$ cascades. The measured precession angles $\omega\tau$ and the deduced g factors are given in Table II. Further details of the experiments, results, and analysis procedures will be published elsewhere. The hyperfine field strength was found from the ^{192}Pt measurement to be $(92 \pm 8)\%$ of that obtained in radioactivity and spin-echo measurements, -123 ± 3 T [2,9]. To interpret such diminutions, it is conventional to assume a two-site model in which a fraction of the implanted nuclei reside on zero-field sites. It is likely, however, that the nuclei on interstitial or damaged sites have a reduced but nonzero field [10]. We have analyzed our data with the two-site model, considering several alternative assumptions about the fractions of nuclei at partial- and full-field sites, subject to the constraint that the effective field is 92% of the full value. The differences in the extracted precession angles were always small compared with other sources of uncertainty.

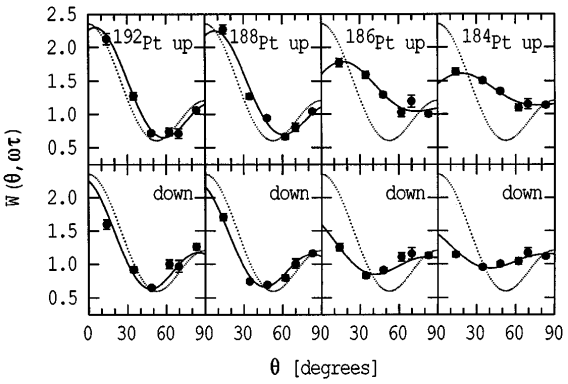

FIG. 1. Measured and fitted perturbed $0_2^+ \rightarrow 2_1^+ \rightarrow 0_1^+$ angular correlations. The unperturbed angular correlations (dotted lines) are also shown.

TABLE II. Measured precession angles and g factors.

Nuclide	$E(2_1^+)$ (keV)	I_i [a]	E_γ [a] (keV)	$\omega\tau(2_1^+)$ (mrad)	$\tau(2_1^+)$ [b] (ps)	$g(2_1^+)$
^{192}Pt	316.5	0_2^+	878.7	104 ± 12		
		2_2^+	296.0	113 ± 9		
		3_1^+	604.4	120 ± 30		
				110 ± 7 [c]	62 ± 2	0.30 ± 0.01 [d]
^{188}Pt	265.6	0_2^+	533.4	155 ± 11		
		2_2^+	340.0	189 ± 22		
		3_1^+	670.8	123 ± 42		
				160 ± 10 [c]	93 ± 7	0.29 ± 0.04
^{186}Pt	191.6	0_2^+	279.7	624 ± 53		
		4_1^+	298.6	590 ± 64		
		2_2^+	607.2	522 ± 98		
		3_1^+	765.4	628 ± 105		
				601 ± 35 [c]	375 ± 14	0.27 ± 0.03
^{184}Pt	163.0	0_2^+	329.0	1005 ± 83		
		4_1^+	273.0	804 ± 81		
		6_1^+	362.5	917 ± 138		
				904 ± 53 [c]	543 ± 13	0.28 ± 0.03

[a] Initial level, I_i, and γ-ray energy, E_γ, of transition in coincidence with the $2_1^+ \rightarrow 0_1^+$ transition.

[b] Lifetimes from Refs. [6–8].

[c] Weighted average.

[d] Calibration value adopted from [3].

The results presented in Table II are for the case where no field acts on 8% of the implants. At most, the alternative assumptions increase $g(2_1^+)$ in ^{184}Pt by ~4%. If the ^{192}Pt measurement were ignored and the hyperfine field from the literature [2,9] adopted, the g factors would all decrease by 8%.

We will discuss the g factors of the Pt isotopes in relation to (i) global experimental trends, (ii) previous theoretical work, (iii) shape coexistence, and (iv) the interacting boson model.

Figure 2 shows the experimental $g(2_1^+)$ values for nuclei between ^{152}Gd and ^{198}Pt, which have $50 \leq Z \leq 82$ and $82 \leq N \leq 126$. Comparisons are made with benchmark estimates of the geometrical model (GM) [11] and the proton-neutron interacting boson model (IBM-2) [12]. In the GM $g_{\rm GM} \sim Z/A$, while in the F-spin symmetric limit of IBM-2

$$g_{\rm IBM} = g_\pi N_\pi/N_t + g_\nu N_\nu/N_t\,, \qquad (2)$$

where $N_{\pi(\nu)}$ is the number of proton (neutron) bosons and $N_t = N_\pi + N_\nu$. Since the boson g factors are $g_\pi \sim 1$ and $g_\nu \sim 0$, $g_{\rm IBM} \sim N_\pi/N_t$. In the upper half of a valence neutron shell, where the bosons are *holes,* these two models initially predict the opposite mass dependence for the g factors in a sequence of collective isotopes. At the next level of sophistication, the inclusion of pair correlations in the GM tends to reduce $g_{\rm GM}$ to about $0.7Z/A$ [13], while the boson g factors may be treated as empirical parameters (typical values $g_\pi = 0.65$, $g_\nu = 0.05$, cf. [14]).

Kumar and Baranger (KB) [15] performed an extensive theoretical study of rare-earth and transitional nuclei in which they calculated the parameters of the geometrical model Hamiltonian microscopically using the pairing-plus-quadrupole interaction. Their g factors, shown in Fig. 2, were calculated in the cranking formalism. KB predicted that the transition from prolate to oblate deformations in the Pt isotopes lies between ^{188}Pt and ^{190}Pt in agreement with the more recent work of Bengtsson *et al.* [16]. It is evident from Fig. 2 that the work of KB, the IBM-2 estimates, and the global experimental trends all suggest that the g factors of the Pt isotopes might decrease toward mid-shell ($N = 104$). Instead, they remain almost constant, agreeing with $g \sim 0.7Z/A$ (although the mass variation is in the opposite sense).

Sprung *et al.* [17] have calculated g factors for selected Pt isotopes, also using the cranking formalism, but with density-dependent Hartree-Fock wave functions. The g factors in ^{184}Pt and ^{188}Pt were calculated for both prolate and oblate shapes. As shown in Fig. 3, the g factors of KB for (prolate) $^{184-188}$Pt do not agree with those for prolate shapes calculated by Sprung *et al.* As g factors calculated in the cranking approach can be very sensitive to the pairing parameters and the adopted single-particle spectra, which in turn are affected by the nuclear shape, it would be timely to reexamine these calculations in light of the new data.

The neutron-deficient Pt isotopes have low-excitation level structures that are indicative of shape coexistence [16,18,19]. Along with the ground band, there is another $K^\pi = 0^+$ band built on a low-lying 0^+ state. The observed states can be interpreted in terms of the interaction between two coexisting configurations, one prolate deformed and the other oblate but near spherical. As the energies of the 0_2^+ states are known, the degree of mixing

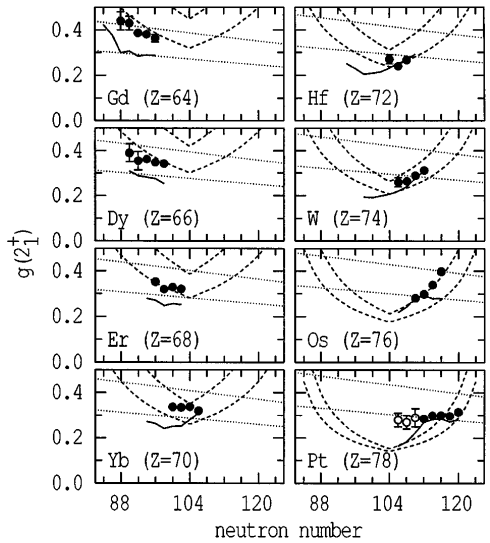

FIG. 2. Systematics of 2_1^+ state g factors in nuclei with $50 \leq Z \leq 82$ and $82 \leq N \leq 126$. The dashed lines are IBM-2 estimates [Eq. (2)] with $g_{\pi(\nu)} = 1(0)$ and $g_{\pi(\nu)} = 0.65(0.05)$. The dotted lines show Z/A and $0.7Z/A$. Solid lines are from Kumar and Baranger [15]. Previous experimental data are tabulated in Refs. [3,25].

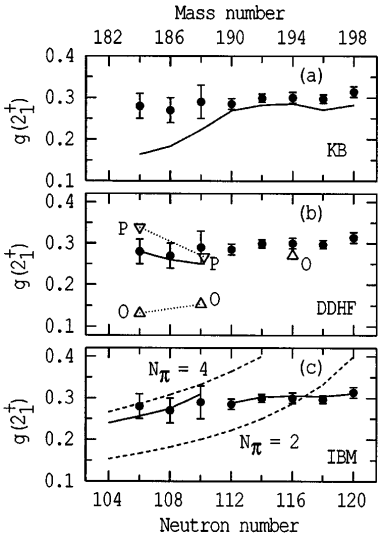

FIG. 3. Comparison of experimental and theoretical g factors in $^{184-198}$Pt: (a) Kumar and Baranger [15]. (b) Density-dependent Hartree Fock calculations for prolate (P) and oblate (O) shapes [17]. The solid line indicates the present two-band mixing results (see text). (c) IBM-2 in the F-spin symmetry limit for the "normal," $N_\pi = 2$ (same as the upper dashed curve in Fig. 2) and "deformed," $N_\pi = 4$ configurations. The solid lines are F-spin mixed calculations for $^{190-198}$Pt [3], and the present band-mixing results for $^{182-188}$Pt.

between the coexisting structures can be determined from the level scheme. Once the unperturbed ground state energy has been found by fitting the high-spin states in the ground band, the interaction strength may be extracted [18], and, assuming it is spin independent, the wave functions determined for the excited states. Observed $E2$ transition rates [7,18] and $E0$ transitions in ^{184}Pt [20] are in accord with such empirical wave functions. Recently, a series of decay measurements on the spectroscopies of ^{178,180,182}Pt has been interpreted using three-band mixing (a quasi-γ band is included) [21]. To estimate the g factors, however, we will use the simpler two-band approach [18]. From fits to the level schemes we find that the deformed configuration dominates the wave functions of the 2_1^+ states in $^{182-188}$Pt, i.e., $\sim$70% to 80% amplitude squared. (We have included ^{188}Pt in this analysis although it is believed to be γ soft [16].) Adopting the g factors of Sprung *et al.* [17] as the g factors of the unperturbed prolate and oblate contributions to the wave function, we obtain the g factors shown by the solid line in Fig. 3(b). Agreement with experiment is good, with $g(2_1^+)$ determined predominantly by the deformed configuration.

From the perspective of the IBM, the g factors can be sensitive to F-spin mixing [22] and/or variations in the number of effective valence protons [14]. Recently it has been shown [3,23] that the $M1$ properties and g-factor systematics of the low-lying states in $^{186-192}$Os and $^{190-198}$Pt can be described using a simple IBM-2 Hamiltonian with appropriate F-spin breaking. To explain the g factors of the Pt isotopes with $A < 190$ by this mechanism, however, would require a negative energy for the proton d boson. Rather, the deformed (prolate) structure which dominates the wave functions of the 2^+ states has a configuration in which at least one pair of protons is promoted across the $Z = 82$ shell gap into the deformation-driving $h_{9/2}$ orbital [16,19]. It also contains extra neutron pairs [16], but these have less influence on the magnetic moment. As a first approximation then, the prolate configuration has six proton holes and two proton particles, implying two more proton bosons than the normal (four proton-hole) configuration. In Fig. 3(c), the g factors calculated in the F-spin limit of the IBM are shown for the spherical configuration ($N_\pi = 2$), for the deformed configuration ($N_\pi = 4$), and for the shape-mixed combination with the mixing amplitudes described above. The measured g factors support the interpretation that the deformed states have an enlarged proton boson number and are consistent with the shape-coexistence model. The proton-neutron IBM therefore provides a phenomenological description of g factors in the transitional Pt isotopes in terms of F-spin mixing ($A \geq 190$) and boson-number effects ($A < 190$). A consistent description might model both processes through $A = 190$ by means of mixed-configuration IBM calculations like those performed for the Hg nuclei [24].

In conclusion, we have demonstrated that magnetic moment systematics for short-lived excited states can be extended across a long chain of isotopes that includes neutron-deficient nuclei far from stability. In the transitional Pt nuclei the measured $g(2_1^+)$ values remain remarkably constant, contrary to expectations that they might decrease markedly near the middle of the valence neutron shell. The g factors are consistent with shape-coexistence models in which the deformed configuration has an increased number of active protons.

We are grateful to our colleagues T. Kib'edi, P. H. Regan, A. M. Baxter, P. M. Walker, and B. Fabricius for assistance with the experiments. One of us (A. E. S.) is supported by the Australian Research Council.

[1] E. Recknagel, *Nuclear Spectroscopy and Reactions*, edited by J. Cerny (Academic Press, New York, 1974), Pt. C, p. 93.
[2] E. Bodenstedt *et al.*, Z. Phys. A **342**, 249 (1992).
[3] S. S. Anderssen, A. E. Stuchbery, and S. Kuyucak, Nucl. Phys. **A593**, 212 (1995).
[4] G. D. Dracoulis and A. P. Byrne, Department of Nuclear Physics Annual Report No. ANU-P/1052, Australian National University, 1989, p. 115 (unpublished).
[5] A. P. Byrne, P. M. Davidson, and G. D. Dracoulis, Department of Nuclear Physics Annual Report No. ANU-P/1101, Australian National University, 1991, p. 158 (unpublished).
[6] S. Raman *et al.*, At. Data Nucl. Data Tables **36**, 1 (1987).
[7] U. Garg *et al.*, Phys. Lett. B **180**, 319 (1986).
[8] S. S. Anderssen, Ph.D. thesis, Australian National University, 1995 (unpublished).
[9] M. Kontani and J. Itoh, J. Phys. Soc. Jpn. **22**, 105 (1967).
[10] A. E. Stuchbery, S. S. Anderssen, and E. Bezakova, Hyperfine Interact. (to be published).
[11] A. Bohr and B. Mottelson, *Nuclear Structure* (Benjamin, New York, 1975), Vol. 2.
[12] F. Iachello and A. Arima, *The Interacting Boson Model* (Cambridge University Press, Cambridge, 1987).
[13] S. G. Nilsson and O. Prior, Mat. Fys. Medd. K. Dan. Vidensk. Selsk. **32**, No. 16 (1961).
[14] A. Wolf, D. D. Warner, and N. Benczer-Koller, Phys. Lett. **158B**, 7 (1985).
[15] K. Kumar and M. Baranger, Nucl. Phys. **A110**, 529 (1968).
[16] R. Bengtsson *et al.*, Phys. Lett. B **183**, 1 (1987).
[17] D. W. L. Sprung *et al.*, Nucl. Phys. **A326**, 37 (1979).
[18] G. D. Dracoulis *et al.*, J. Phys. G **12**, L97 (1986).
[19] J. L. Wood *et al.*, Phys. Rep. **215**, 101 (1992).
[20] Y. Xu *et al.*, Phys. Rev. Lett. **68**, 3853 (1992).
[21] P. M. Davidson, Ph.D. thesis, Australian National University, 1994 (unpublished); P. M. Davidson, G. D. Dracoulis, T. Kibédi, A. P. Byrne, S. S. Anderssen, A. M. Baxter, B. Fabricius, G. J. Lane, and A. E. Stuchbery (to be published).
[22] A. E. Stuchbery, I. Morrison, and H. H. Bolotin, Phys. Lett. **139B**, 259 (1984).
[23] S. Kuyucak and A. E. Stuchbery, Phys. Lett. B **348**, 315 (1995).
[24] A. B. Barfield *et al.*, Z. Phys. A **311**, 205 (1983).
[25] A. E. Stuchbery, Nucl. Phys. **A589**, 222 (1995).